JOURNAL OF MATERIALS SCIENCE **37** (2002) 203–209

The effect of test temperature on the intergranular cracking of Nb-A286 alloy in low cycle fatigue

B. S. RHO, S. W. NAM*
Department of Materials Science and Engineering, Korea Advanced Institute of Science and Technology, 373-1 Kusong-dong Yusong-gu, Taejon, 305-701, Korea
E-mail: namsw@kaist.ac.kr

X. XIE
High Temperature Materials Research Laboratory, University of Science and Technology Beijing, Beijing 100083, People's Republic of China

The continuous low cycle fatigue behaviors of a Fe-base superalloy, Nb-modified A286 alloy, have been evaluated at the test temperatures of 650°C and 350°C under various total strain ranges. It was found that the change of the slope in the Coffin–Manson plot was closely related to the fatigue cracking with the test temperature. In the high temperature low cycle fatigue (HTLCF) of Nb-A286 alloy, the fatigue cracking exhibited the intergranular mode at 650°C and the transgranular mode at 350°C. The intergranular fatigue cracking at 650°C was due to the precipitation of the η phase at the grain boundary assisted by the applied stress during low cycle fatigue. It is investigated whether the η precipitate at the grain boundary provides the site for the grain boundary cavitation, which induces the intergranular cracking in low cycle fatigue. This is confirmed by the results of low cycle fatigue at 25°C after heat treatment which forms the η phase at the grain boundary.

1. Introduction

The iron-base superalloy A286 is widely used for jet engine parts in intermediate temperature regions. It is nominally a 25Ni-15Cr austenitic alloy containing Ti and Al additions. It is strengthened by an aging treatment which precipitates the ordered fcc γ' phase, Ni_3(Ti, Al). However, the relatively low strength of this alloy restricts its extensive use in parts that require high strength during high temperature service. Recently, by adding Nb element, the modified A286 has been developed. It is reported that the addition of Nb element to the iron-base superalloy increases the amounts of γ' phase, the main strengthener, and improves the stability of γ' phase to give higher strength, longer fatigue life and creep-rupture time than those of commercial A286 alloys [1].

Many superalloys are generally subjected to cyclic loading at elevated temperature service. During low cycle fatigue tests the microstructure of a material may be differently changed due to the fatigue deformation under different test temperatures. Such microstructural changes affect the fatigue cracking in a different way with the test temperature. It has generally been reported that as the temperature increases, the fracture mode changes from the transgranular to the intergranular cracking to shorten the fatigue life. This is due to the rapid crack propagation rate in the case of the intergranular cracking. Furthermore, the change from the transgranular to the intergranular cracking mode in fatigue is caused by the cycling frequency effect [2], the environment effect [3, 4], and the tensile hold time effect [5–7] in low cycle fatigue. However, the effect of temperature on the cracking under high temperature low cycle fatigue (HTLCF), and the mechanisms of the fatigue cracking caused by the change of the microstructure with service temperature in the newly developed Nb-A286 alloy are not yet clearly understood.

For the sake of safety and better performance, the evaluation of the mechanical properties of materials under real application conditions is very valuable and necessary. Therefore, it is important to investigate the effect of temperature on the mode change of the cracking with temperature. The mechanism of the intergranular cracking of Nb-modified A286 alloy under high temperature low cycle fatigue will be also discussed.

2. Experimental procedure

The chemical composition and heat treatment schedule of the Nb-A286 iron base superalloy used in this investigation are shown in Table I.

*Jointly Appointed at the Center for the Advanced Aerospace Materials.

TABLE I The chemical composition and heat treatment of Nb-A286 alloy (in wt%)

C	Mn	Si	P	S	Cr	Ni	W	Mo	V	Al	Ti	Nb	Fe
0.052	0.07	0.02	0.012	0.005	13.75	28.75	0.92	1.63	0.2	0.21	2.25	0.47	Bal.

980°C/1 hr/oil quench
710°C/16 hrs/air quench

Cylindrical specimens used for this research have been machined to have 8 mm gage length and 7 mm diameter. After machining, the specimens were polished with emery paper of various grades from 220 to 2000 grit to remove machining-related surface defects and to make a mirror surface. Using the well-polished specimens, fatigue tests were conducted in an axial total strain control user fully reversed push-pull loading ($R = -1$) in a servohydraulic testing machine, Instron 1350. Fatigue tests were carried out at the temperatures of 350°C and 650°C in an air atmosphere. The symmetric triangular strain wave shape was used with a total strain rate of 4×10^{-3}/s to conduct continuous low cycle fatigue tests for the total strain range of $\pm 1.0 \sim \pm 2.7\%$. The fatigue life (N_f) is defined as the number of cycles at which the saturated tensile load is dropped by 20% [8].

For high temperature fatigue tests, a dual elliptical radiant heater was used to heat the specimen and the temperature was maintained within the accuracy of ±5 K as measured on the top and center of the gauge section. The axial strain was measured using an extensometer attached at the specimen holder situated outside the radiant heater because the gauge section was surrounded by the heating chamber. For the strain calibration at room temperature, two extensometers are used; one is installed at the specimen holder for strain control, and the second one is attached within the gauge length to measure the strain. At the high temperature, however, the measurement of the strain in the gauge length is not possible because of the furnace. However, it is thought that, since the specimen gauge length is heated to the highest temperature and has the smallest cross-section, the validity of the strain measurement at room temperature is reliable at the test temperature [9].

Some of the fatigued specimens were chosen to investigate the fatigue fracture surface and deformation microstructures. A scanning electron microscope (SEM, JEOL JSM 840A) and transmission electron microscope (TEM, Philips CM20) were used to observe the fatigue fracture surface, fatigue cracking, and the microstructure, respectively.

3. Results and discussion

3.1. Microstructure prior to low-cycle fatigue test

Fig. 1 shows the microstructure of Nb-A286 alloy observed by optical microscopy before the fatigue test. It is observed that the size of the grains is about 60–100 μm. Even though other workers have observed Ti oxide, Ni_3Ti-η phase and σ phase in the alloys having the similar compositions of Nb-A286 alloy [10, 11], these phases were not observed in the alloy used in this study because of the proper control of the alloy composition and heat treatment in order to avoid the detrimental phases on the mechanical properties in this alloy.

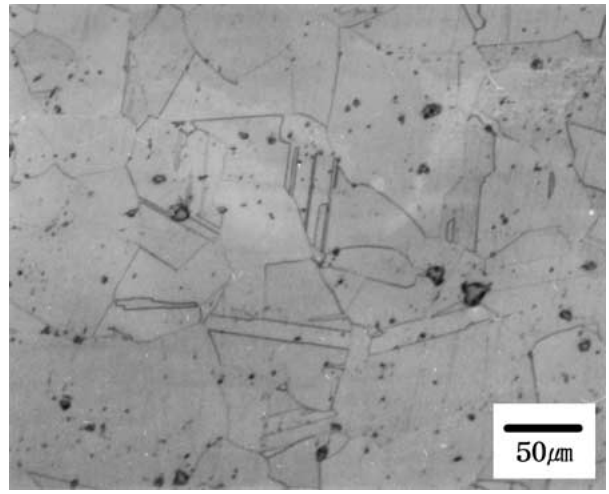

Figure 1 Optical microstructure of Nb-modified A286 alloy before the fatigue test.

3.2. Low cycle fatigue behaviors at 650°C and 350°C

All the data for continuous low cycle fatigue of the investigated Nb-A286 alloy are plotted in Fig. 2 as a function of plastic strain range ($\Delta\varepsilon_p$) and temperature. The values of plastic strain range for the Coffin-Manson plot were taken from hysteresis loops corresponding to half life ($N_f/2$). As shown in Fig. 2, it can be known that fatigue life decreases with increasing plastic strain

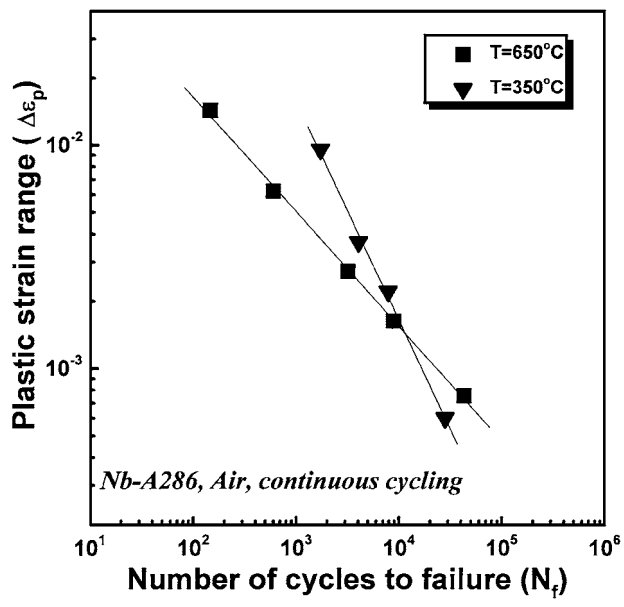

Figure 2 Relationship between plastic strain range and fatigue life, Coffin-Manson plot.

range at a fixed temperature, and the fatigue life at a higher value of plastic strain range also decreases with increasing test temperature, while the fatigue life at a low value of plastic strain range increases with increasing test temperature.

For the most materials, when the fracture mechanism is identical, the slope in the Coffin-Manson plot has some tendency to be parallel regardless of the test temperature or to become steeper as the test temperature increases. The reason for this phenomenon is due to the additional creep properties with increasing temperature and increasing the exposure time of high temperature under low plastic strain range, followed by the decrease of fatigue life. But, these trends are not observed in the results of low cycle fatigue of this investigation with Nb-A286 alloy. From the results of Fig. 2, it can be seen that the slope in the Coffin-Manson plot under the condition of 650°C is less steep than that under the condition of 350°C. A similar result has been found in the result of other investigators [12]. They might report that the peculiar change of the slope with temperature in the Coffin-Manson plot of IN718 alloy is associated with the change in deformation mode as well as the increased environmental effects at the elevated temperature. However, the reason for this change of the slope in the Coffin-Manson plot is not clearly understood.

To clearly understand the cyclic response of the Nb-A286 alloy, the tensile peak stress is plotted in Fig. 3 against N/N_f, where N represents the cycle number and N_f the cycles to failure. From Fig. 3, it can be seen that at the test temperature of 650°C, the alloy generally exhibits initial cyclic softening if the imposed total strain ranges are higher than ±2.0%, and the extent of softening increases with the increase in total strain range. It has been reported that this cyclic softening phenomenon was explained by many mechanisms: precipitation dissolution [13], disordering of precipitates [14], overaging [15], and precipitate size reduction [16]. The explanation of these mechanisms has implied that cyclic softening was mainly due to the interaction between the precipitate and dislocations. It can also be known from Fig. 3 that the alloy shows the different cyclic stress response behavior which depends on the total strain range at the test temperature of 350°C. At the test temperature of 350°C and two lower total strain ranges of ±1.7 and ±2.0%, a stable cyclic stress response behavior is observed after the alloy is hardened to a maximum stress level, while above the total strain range of ±2.3%, the stability of cyclic stress response is observed from the beginning of initial cycle. It has been reported that the cyclic stress response of GH4049 alloy is mainly dependent upon the strain amplitude, and that cyclic hardening or initial hardening followed by softening are observed at higher strain amplitudes while the alloy shows a fairly stable cyclic stress response at lower strain amplitudes [17]. Therefore, it seems that the cyclic stability of the Nb-A286 alloy and this kind of Ni-Fe base superalloy in low cycle fatigue is dependent upon the testing temperature and the imposed total strain range.

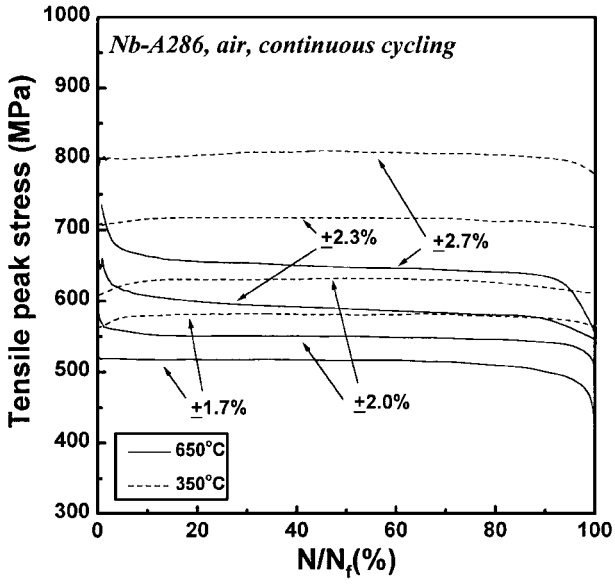

Figure 3 Cyclic stress response as a function of the test temperature and strain range.

3.3. Fatigue fracture surfaces and microstructures after low cycle fatigue

The fatigue fracture surfaces are shown in Figs 4a and 5a for the test temperatures of 650°C and 350°C,

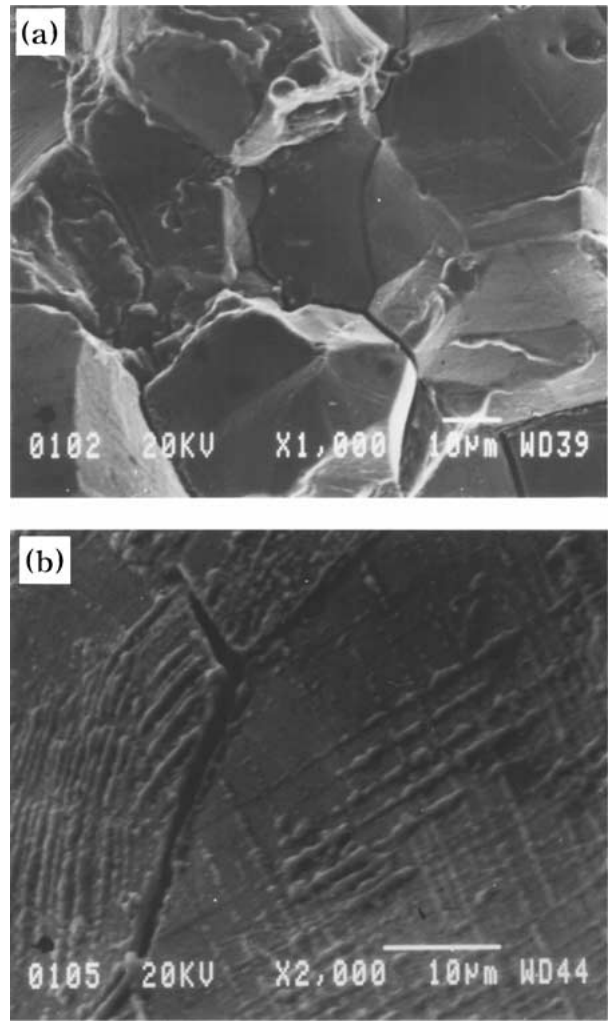

Figure 4 SEM micrographs showing (a) the fatigue fractured surface and (b) the specimen surface after fatigue fracture of Nb-A286 alloy in the fatigue condition of $T = 650°C$, $\Delta\varepsilon_t = \pm 2.7\%$.

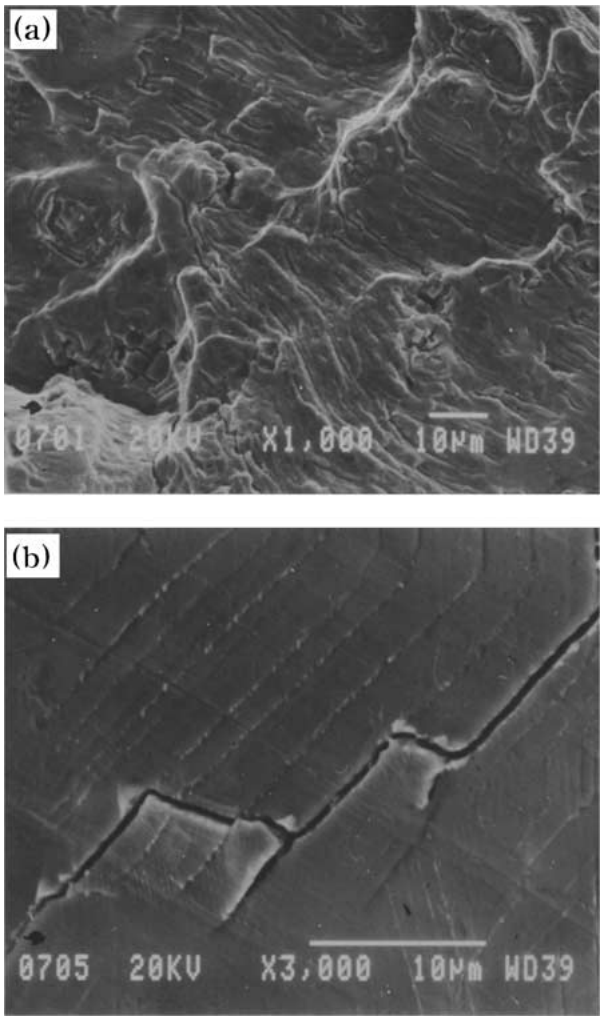

Figure 5 SEM micrographs showing (a) the fatigue fractured surface and (b) the specimen surface after fatigue fracture of Nb-A286 alloy in the fatigue condition of $T = 350°C$, $\Delta\varepsilon_t = \pm 2.7\%$.

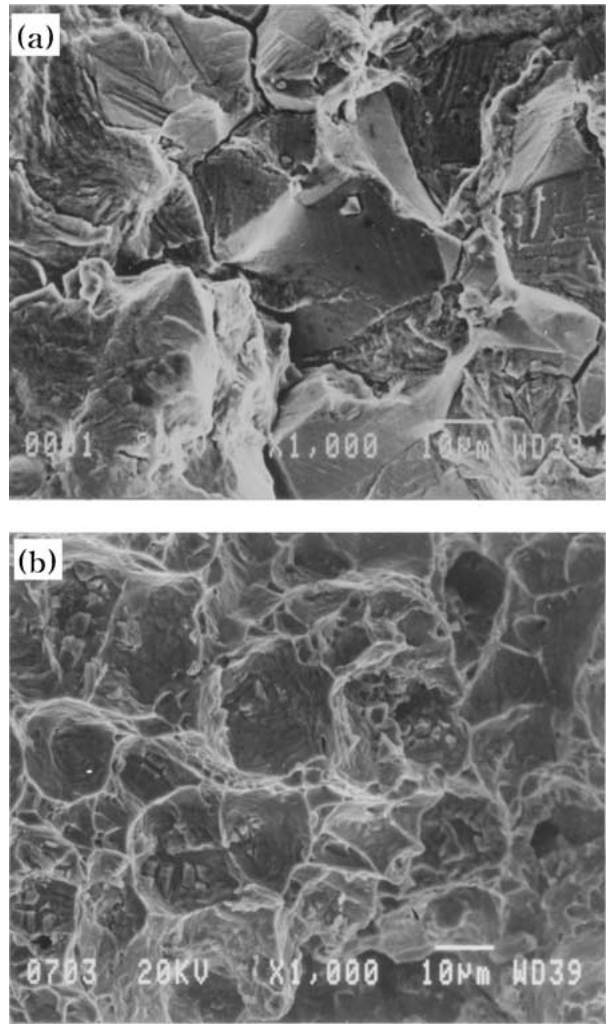

Figure 6 SEM micrographs of the fractured surface by impact at LNT after low cycle fatigue of Nb-A286 alloy in the fatigue condition of $\Delta\varepsilon_t = \pm 2.7\%$. (a) $T = 650°C$ and (b) $T = 350°C$.

respectively. A noticeable difference is found in the fatigue fracture mode with test temperature. In Fig. 4a, it can be observed that the fatigue crack propagation mode is intergranular in the test condition of 650°C, while in Fig. 5a the transgranular mode which shows the typical striations is observed in the test condition of 350°C. Figs 4b and 5b show the surface of the fatigued specimens at the test temperature of 650°C and 350°C, respectively. Fig. 4b exhibits the fatigue cracks initiated along the grain boundary, growing the intergranular cracking toward the interior region of the specimen. But, it can be observed in Fig. 5b that the fatigue cracks are initiated along the slip traces, that is, at the interior regions of the grain, inducing the transgranular cracking. This implies that the cracking mode in low cycle fatigue is dependent upon the test temperature, and higher test temperature affects the weakness of the grain boundary compared with the matrix.

Generally, it is well known that, depending on the test temperature, there are numerous damage mechanisms for different fracture modes. Among many factors affecting the fatigue crack mode, grain boundary oxidation has been considered as the most important factor to determine the possibility of the intergranular cracking at the elevated temperature. It has been reported that in the Ni-base superalloy the crack propagation mode is closely related to the testing temperature, and the transition from transgranular to intergranular fracture is promoted with increasing temperature due to creep and oxidation [17]. However, in Fig. 6 which shows the fracture surface by impact at liquid nitrogen temperature (LNT) after low cycle fatigue test, it can be seen that the fracture surfaces at 650°C and 350°C exhibit the intergranular and transgranular fracture, respectively. This means that, since the interior region of the specimen under low cycle fatigue is not affected by being exposed under the oxidized atmosphere, the intergranular fracture in the interior region of the fatigued specimen at 650°C cannot be simply explained by the effect of the oxidation on the intergranular crack in high temperature of low cycle fatigue of Nb-A286 alloy. Therefore, even though the intergranular cracking is somewhat accelerated by oxidation, the observation of the intergranular fracture in the interior region of the fatigued specimen indicates that the major reason for the dominance of intergranular cracks is not the oxidation itself but the low fracture strength of the boundary relative to the matrix at the elevated temperature.

Fig. 7 shows the SEM photographs of the sub-surface region of the fatigue fracture surface after low cycle fatigue at 650°C and 350°C. As shown in Fig. 7,

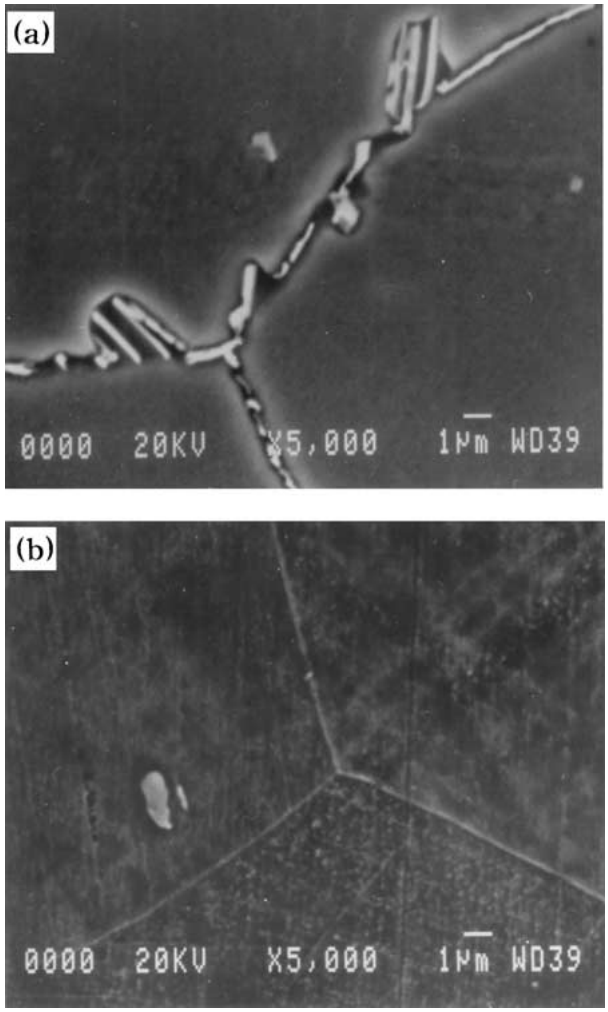

Figure 7 SEM micrographs of the sub-surface region of the fatigue fracture surface after low cycle fatigue in the condition of (a) $T = 650°C$, $\Delta\varepsilon_t = \pm 1.0\%$ and (b) $T = 350°C$, $\Delta\varepsilon_t = \pm 2.0\%$.

the grain boundary precipitates can be observed in the case of 650°C, while no grain boundary precipitates can be observed in the case of 350°C. In order to identify the precipitates at the grain boundary at the test temperature of 650°C, the TEM investigation was conducted using the specimen of low cycle fatigue tested at 650°C. Fig. 8 shows the bright field image and diffraction patterns of the grain boundary precipitate after the low cycle fatigue test of $T = 650°C$ and total strain range $\pm 1.0\%$, and these precipitates spots are analyzed to be corresponding to the Ni_3Ti-η precipitates with the hexagonal close-packed (HCP) structure. In the previous work, it has been studied that the formation of this η phase at the grain boundary under low cycle fatigue is facilitated at a somewhat low temperature due to the accommodation of deformation near the grain boundary, compared with the precipitation temperature of the η phase in consideration of only the thermal effect [18]. It has also been reported that the precipitates at the grain boundary can act as the nucleation site of the crack during the temperature deformation [19–21]. Especially, the formation of this η phase at the grain boundary during heat treatment has been reported to give rise to the increases in intergranular fracture in the tensile test [21]. So, attempts have been made to understand the mechanism of the intergranular cracking in the high temperature low cycle fatigue of Nb-A286 alloy through heat treatment for the formation of the η phase, subsequently followed by the low cycle fatigue test under the condition in which the grain boundary precipitate, η phase cannot be formed.

To understand the effect of the η phase on the intergranular cracking under low cycle fatigue, the heat treatment for 30 hours at 800°C was conducted, followed by air cooling. The microstructure for the heat-treated Nb-A286 is shown in Fig. 9, which exhibits the η precipitates at the grain boundary. But, after the heat treatment, the growth of grains and the formation of other precipitates in the alloy cannot be observed. Using the heat-treated specimen, the low cycle fatigue test was conducted in the condition of $T = 25°C$ and total strain range $\pm 2.7\%$. Fig. 10 shows the fatigue fracture surface of the non heat-treated specimen and heat-treated specimen under the same total strain range in the test temperature of 25°C. As shown in Fig. 10a, the fatigue fracture surface of the non heat-treated specimen reveals the transgranular mode, which is similar to the fatigue fracture surface of 350°C. However, the fatigue fracture surface of the heat-treated specimen which has

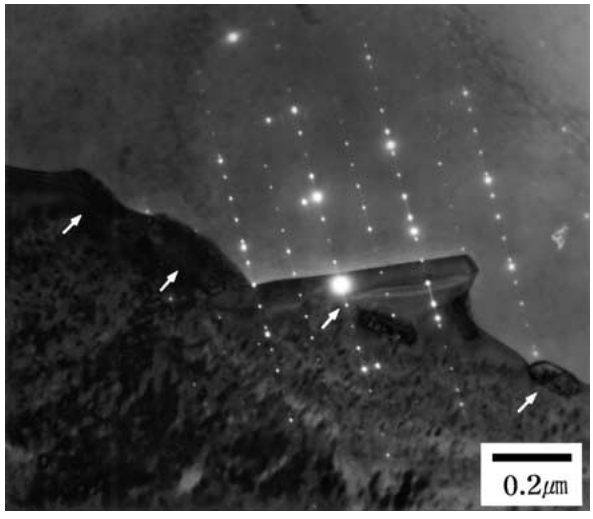

Figure 8 TEM photographs showing the bright field image and the diffraction pattern of the Ni_3Ti-η precipitates at the grain boundary after the low cycle fatigue test of $T = 650°C$, $\Delta\varepsilon_t = \pm 1.0\%$. (B = [011])

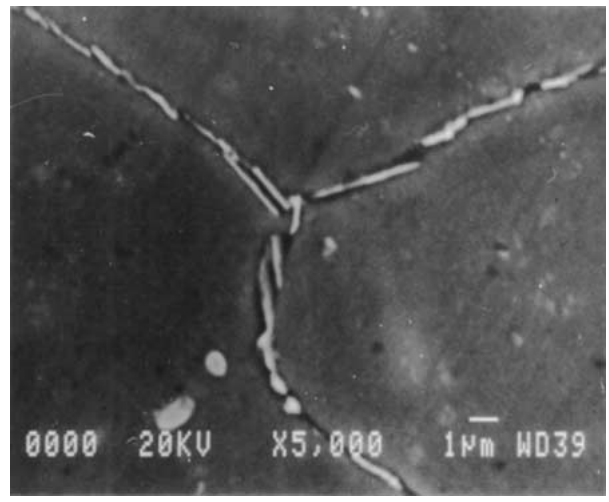

Figure 9 SEM micrograph showing the microstructure with η precipitates at the grain boundary after being heat treated for 30 hours at 800°C.

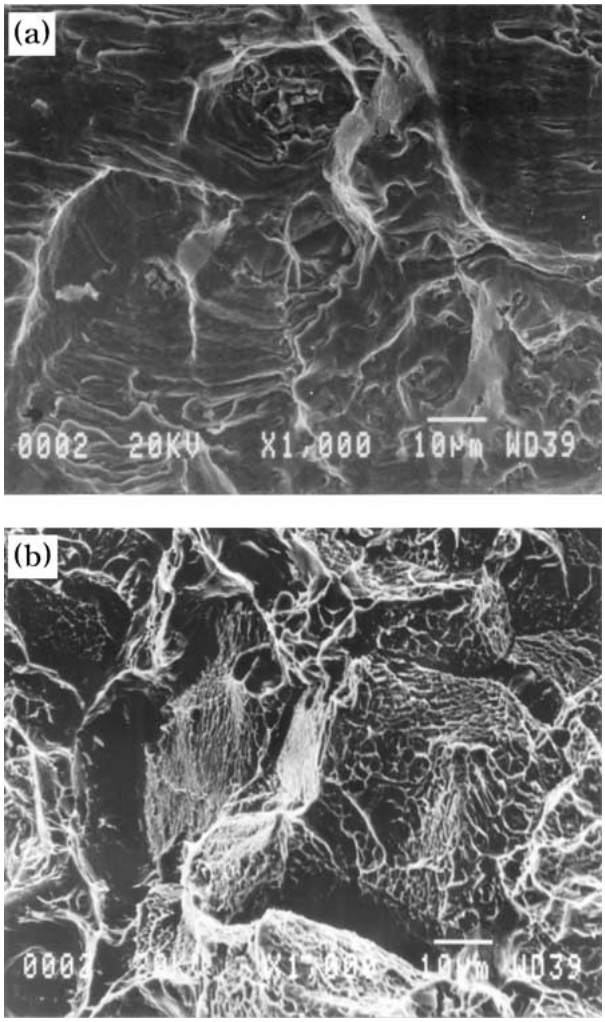

Figure 10 SEM micrographs showing the fatigue fracture surface after the low cycle fatigue test of $T = 25°C$, $\Delta\varepsilon_t = \pm 2.7\%$. (a) non heat-treated specimen and (b) heat-treated specimen.

the η phase at the grain boundary reveals the intergranular mode as shown in Fig. 10b. Also, the mechanical properties of the low cycle fatigue with the presence of the η phase at the grain boundary are tabulated in Table II. The fatigue life of the heat-treated specimen is shorter than that of the non heat-treated specimen, even though there is little difference in the plastic strain range between the heat-treated and the non heat-treated specimen. This indicates that the existence of η precipitates at grain boundary may be very closely related to the intergranular cracking in low cycle fatigue, and the fatigue fracture with the test condition of forming the η phase at the grain boundary has the high tendency to have the intergranular mode, compared with the case of not forming the η phase at the grain boundary. It can also be known that the intergranular cracking due to the presence of the η phase at the grain boundary induces the decrease in fatigue life.

In most instances where such precipitates cause intergranular fracture, small cavities can be formed around the grain boundary precipitates. The growth of these cavities and their eventual link-up by the applied stress cause the crack to proceed along the grain boundaries. Therefore, it can be inferred from this study of Nb-A286 alloy that the formation of the η phase at the grain boundary during high temperature low cycle fatigue plays a dominant role of nucleating the site of the grain boundary cavitation, and the accommodation of deformation near the grain boundary during low cycle fatigue induces the growth of grain boundary cavitation, thereby accelerating the intergranular fatigue cracking of Nb-A286 alloy.

TABLE II The low cycle fatigue properties of Nb-A286 alloy with the existence of the η phase at the grain boundary in the condition of $T = 25°C$, $\Delta\varepsilon_t = \pm 2.7\%$

	$\Delta\varepsilon_p(\%)$	$\Delta\sigma$(MPa)	Hysteresis loop energy (MJ/m^3)	N_f
Heat-treated	1.1	1650	13.1	1847
Non heat-treated	1.1	1550	14.2	2429

4. Conclusions

1) On the low cycle fatigue behaviors of Nb-modified A286 alloy, the decreasing value of the slope of the Coffin-Manson plot for the higher temperature of 650°C in comparison with the case of 350°C is not affected by an oxidation, but by the change in the fatigue cracking mode with the test temperature.

2) The precipitation of the η phase at the grain boundary during low cycle fatigue is thought to provide the site for the grain boundary cavitation which promotes the intergranular failures in high temperature low cycle fatigue of Nb-A286 alloy. This can be confirmed by the results of low cycle fatigue at 25°C after heat treatment which formed the η phase at the grain boundary.

Acknowledgments

The authors would like to express their sincere appreciation to MOST for the financial support of this study (Korean-Chinese joint project, No I-03-112) and special thanks are due to Daye Special Steel Co., Ltd for supplying the material for the specimens.

References

1. G. CHEN, B. WU, L. ZHOU and Y. LI, *Acta Metall. Sinica* **6** (1993) 81.
2. P. RODRIGUEZ and K. BHANU SANKARA RAO, *Progress in Mater. Sci.* **37** (1993) 403.
3. L. F. COFFIN, JR., *Metall. Trans.* **3** (1972) 1777.
4. P. S. MAIYA, *Mater. Sci. Eng.* **47** (1981) 13.
5. J. W. HONG, S. W. NAM and K.-T. RIE, *J. Mater. Sci.* **20** (1985) 3763.
6. S. W. NAM, J. W. HONG and K.-T. RIE, *Metall. Trans. A* **19A** (1988) 121.
7. S. W. NAM, Y. C. YOON, B. G. CHOI, J. M. LEE and J. W. HONG, *Metall. Mater. Trans. A* **27A** (1996) 1273.
8. J. J. KIM and S. W. NAM, *Scripta Metall.* **23** (1989) 1437.
9. D. H. LEE and S. W. NAM, *J. Mater. Sci.* **34** (1999) 2843.
10. T. J. HEADLEY, M. M. KARNOWSKY and W. R. ORENSON, *Metall. Trans. A* **13A** (1982) 345.
11. A. W. THOMPSON and J. A. BROOKS, *ibid.* **6A** (1975) 1431.
12. T. H. SANDERS, JR., R. E. FRISHMUTH and G. T. EMBLEY, *ibid.* **12A** (1981) 1003.
13. A. ABEL and R. K. HAN, *Acta Metall.* **14** (1966) 1495.
14. C. CALABRESE and C. LAIRD, *Mater. Sci. Eng.* **13** (1974) 141.
15. C. A. STUBBINGTON and P. J. E. FORSYTH, *Acta Metall.* **14** (1966) 5.

16. D. FOURNIER and A. PINEAU, *Metall. Trans. A* **8A** (1977) 1905.
17. Z. G. WANG, L. J. CHEN, J. F. TIAN and G. YAO, *Met. & Mater.* **5** (1999) 597.
18. B. S. RHO and S. W. NAM, *Mater. Sci. Eng.,* submitted.
19. P. E. LI, J. S. ZHANG, F. G. WANG and J. Z. JIN, *Metall. Trans. A* **23A** (1992) 1379.
20. A. J. PERRY, *J. Mater. Sci.* **34** (1999) 2843.
21. J. A. BROOKS and A. W. THOMPSON, *Metall. Trans. A* **24A** (1993) 1983.

Received 21 March 2000
and accepted 3 August 2001